International Materials Reviews

ISSN: (Print) (Online) Journal homepage: https://www.tandfonline.com/loi/yimr20

Recent progress in photocatalytic degradation of chlorinated phenols and reduction of heavy metal ions in water by TiO_2-based catalysts

Ayoola Shoneye, Jang Sen Chang, Meng Nan Chong & Junwang Tang

To cite this article: Ayoola Shoneye, Jang Sen Chang, Meng Nan Chong & Junwang Tang (2022) Recent progress in photocatalytic degradation of chlorinated phenols and reduction of heavy metal ions in water by TiO_2-based catalysts, International Materials Reviews, 67:1, 47-64, DOI: 10.1080/09506608.2021.1891368

To link to this article: https://doi.org/10.1080/09506608.2021.1891368

Published online: 28 Feb 2021.

INTERNATIONAL MATERIALS REVIEWS
2022, VOL. 67, NO. 1, 47–64
https://doi.org/10.1080/09506608.2021.1891368

Recent progress in photocatalytic degradation of chlorinated phenols and reduction of heavy metal ions in water by TiO_2-based catalysts

Ayoola Shoneye [a], Jang Sen Chang[b], Meng Nan Chong[b] and Junwang Tang [a]

[a]Department of Chemical Engineering, University College London, London, UK; [b]School of Engineering, Chemical Engineering Discipline, Monash University Malaysia, Selangor Darul Ehsan, Malaysia

ABSTRACT

Among the various semiconductor photocatalysts reported so far, TiO_2 is still the most promising material for real applications because of its excellent chemical and thermal stability, non-toxicity, low cost and highly oxidising photogenerated holes. This review summarises the recent progress (mainly over the last five years) in photocatalytic oxidation of non-biodegradable organic pollutants (chlorophenols) and reduction of toxic heavy metal ions in aqueous solution. The review details the recently developed strategies for improving the performance of TiO_2-based photocatalysts, with particular respect to the visible light activity, charge separation efficiency, stability, separability and adsorption capacity for the remediation of the aforementioned categories of water contaminants, as these factors heavily affect the practical application of this technology. Next, the underlying semiconductor photocatalytic mechanisms have been thoroughly addressed experimentally and theoretically, together with the proposed defect engineering to improve the photocatalytic performance. Finally, the prospect of TiO_2 photocatalysis was discussed.

ARTICLE HISTORY
Received 26 July 2020
Accepted 12 February 2021

KEYWORDS
Photocatalysis; water treatment; TiO_2-based catalysts; heavy metal; chlorophenols

Introduction

Access to potable water is one of the biggest challenges globally, especially in developing countries. Several persistent organic pollutants (pharmaceuticals, pesticides, personal care products, endocrine disrupters) are frequently detected in wastewater effluents [1–3]. Chlorophenols (CPs) and their metabolites are common and recalcitrant environmental pollutants, believed to have high bioaccumulation capability and carcinogenic effect. Figure 1 shows four major CPs (2-CP, 2,4-DCP, 2,4,6-TCP and PCP) that have been classified as first-degree toxic pollutants by the US Environmental Protection Agency (EPA 2003) [4,5].

Adverse effects of phenolic compounds on the human nervous system have been reported and linked to several health disorders, e.g. kidney failure, liver and lung damage [4–6]. CPs find extensive application in the chemical, forestry and wood-working industries. They are used as herbicides, insecticides, fungicides, wood preservatives and chemical intermediates [4,7–10]. Generally, these organic pollutants are released into the environment because of several man-made activities including water disinfection, waste incineration, uncontrolled use of pesticides and herbicides and as byproducts in the bleaching of paper pulp with chlorine [11].

It is interesting to note that 2-CP, 4-CP, 2,4-DCP and 2,4,6-TCP are the most significant CPs formed as byproducts of water chlorination [12,13]. Effluents from a pulp and paper mill were analysed before treatment and subsequent discharge into the Lake Baikal in Russia, 2,4-DCP concentration of (630 ± 50) μg L^{-1}, 2,4,5-TCP concentration of (2660 ± 210) μg L^{-1} and 2,4,6-TCP concentration of (320 ± 30) μg L^{-1} were reported [14]. After treatment, the individual chlorinated phenols were present in trace quantities, except for 2,4,5-TCP with the concentration of (560 ± 50) μg L^{-1} [14]. Environmental pollution agencies and health organisations recommended a maximum allowable concentration for chlorinated phenols as: 0.1 μg L^{-1} in drinking water and 200 μg L^{-1} in wastewater [12].

Various strategies have been employed to remove CPs from the environment, as shown in Table 1. Conventional methods include coagulation-flocculation, reverse osmosis, active carbon adsorption, biodegradation, air stripping and incineration. However, these techniques have some drawbacks and limitations, e.g. toxic byproduct generation, incomplete mineralisation, low efficiency, high energy and capital cost [12–14,16]. CPs absorb light of wavelength below 300 nm; thus, they do not undergo direct sunlight photolysis. Also, they are difficult to decompose completely to CO_2 and HCl by conventional methods due to high stability of the benzene ring [17]. Therefore, it is important to find innovative and cost-effective

CONTACT Junwang Tang junwang.tang@ucl.ac.uk Department of Chemical Engineering, University College London, London WC1E7JE, UK

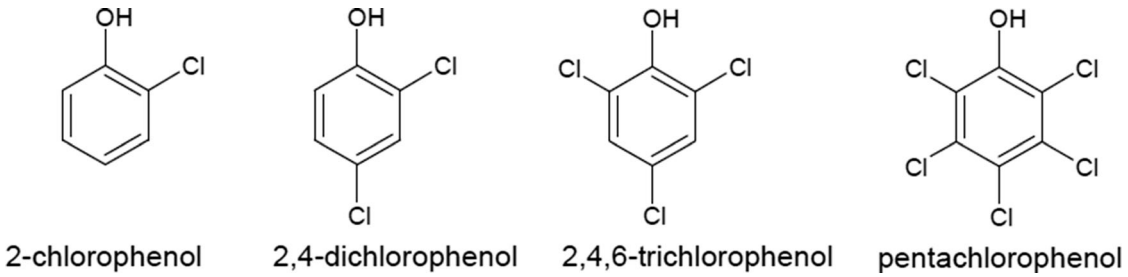

Figure 1. Chemical structure of major common chlorinated phenols.

techniques for the safe and complete degradation of chlorinated organic pollutants such as CPs.

The current trend in wastewater treatment has moved from simple phase transfer to the destruction of pollutants such as by advanced oxidation processes (AOPs). These techniques involve reactive free radical species for non-selective mineralisation of organic compounds to harmless end products. The AOPs are generally based on the generation of the hydroxyl radicals (·OH), which have a great oxidation power, thus can almost oxidise all organic compounds to carbon dioxide and water [15]. There are several methods for generating hydroxyl radicals, e.g. Fenton-based processes, UV-based processes, Ozone-based processes and Photocatalytic processes [16,18–20].

In spite of the advantages of AOPs, there are several limitations in their use: (a) costs may be higher than competing technologies because of energy requirements, (b) harmful intermediates may be formed, (c) pre-treatment of the wastewater may be required to minimise cleaning and maintenance of UV reactor and quartz sleeves, (d) handling and storage of ozone and hydrogen peroxide require special safety precautions and (e) major challenges for the photocatalytic process are catalyst deactivation, slow kinetics, low photo efficiency and unpredictable mechanism [21]. However, AOPs are still more effective than the other techniques for wastewater treatment containing toxic and persistent pollutants [15].

Recently, application of titanium dioxide photocatalytic oxidation technology in environmental remediation has gained considerable attention as a cheap and clean alternative, though there are still various challenges to be resolved for its commercialisation. A high number of organic compounds (dyes, drug residues, pesticides and herbicides) have been eliminated from aquatic environment via TiO_2 photocatalysis [22–25]. Complementary to the reviews published before, this review only concentrates on the progress of TiO_2 photocatalysis over the past five years, thus providing a comprehensive view of the very recent progress in this field.

Table 1. Conventional approaches for the removal of chlorinated phenols [15].

Treatment approach	Drawbacks
Biological treatment	Very slow, incomplete degradation and byproducts may be more toxic than the contaminants
Adsorption technology	Expensive, due to regeneration of the adsorbent materials and post-treatment of solid wastes
Chemical precipitation	Expensive, due to high dosage of chemicals and it produces large quantity of sludge which need post-treatment
Air stripping	High capital cost due to off-gas treatment, aesthetic constraints and technically not reliable

Basic principles of TiO_2 photocatalysis and applications

This review addressed the background in photocatalysis, and the removal of wastewater contaminants, via irradiation of semiconductors (e.g. nano-TiO_2) with a light of energy higher than its bandgap energy (Figure 2). This is the first step in photocatalysis. Subsequently, the excitation of photogenerated electrons into the conduction band takes place, leaving behind energetic photogenerated holes in the valence band. Oxidation reaction is initiated in the valence band, while reduction reaction is initiated in the conduction band of the semiconductor. This requires the semiconductor to have proper band alignment required for organic pollutant decomposition (Figure 3), e.g. the conduction band minimum (CBM) should be higher (more negative in potential) than the redox potential for oxygen reduction to superoxide radicals, and its valence band maximum (VBM) should be lower (more positive in potential) than the redox potential for water or hydroxyl ion oxidation to hydroxyl radicals [13,27,28].

TiO_2 as a photocatalyst

One of the most important aspects of environmental photocatalysis is the availability of an efficient

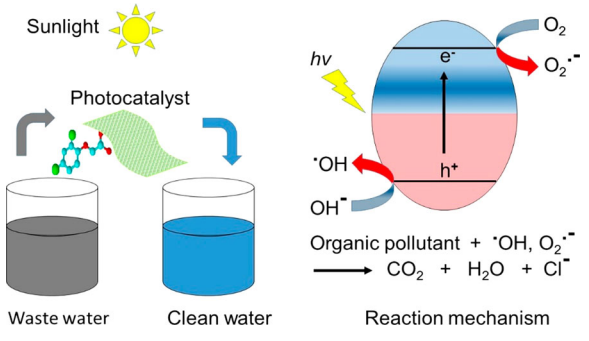

Figure 2. Diagram illustrating the principle of semiconductor photocatalysis for wastewater treatment.

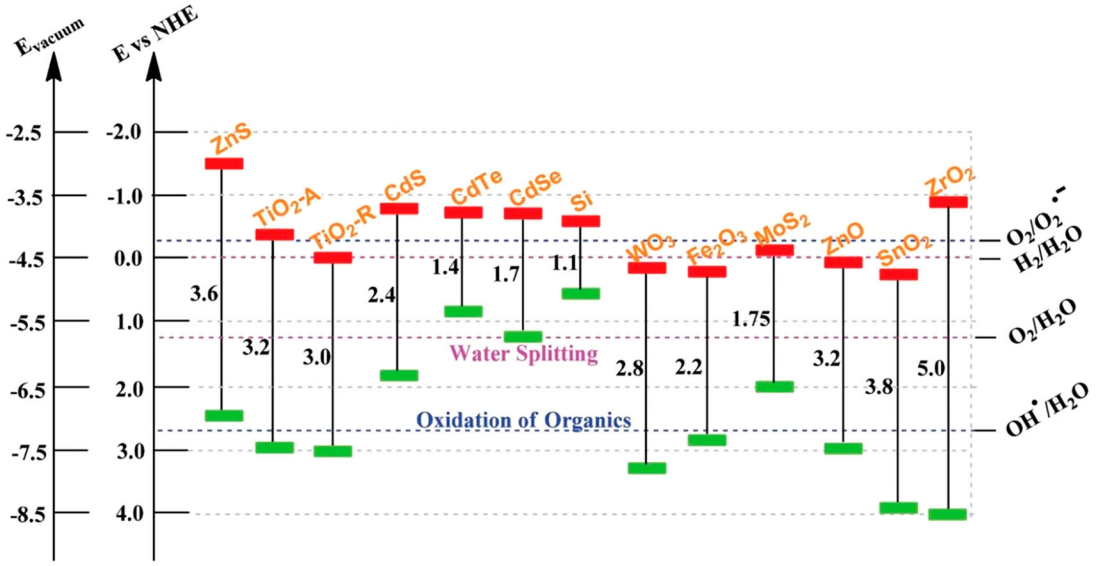

Figure 3. Diagram illustrating the bandgap energy, VB and CB positions of reported efficient semiconductors. Adapted from Wu et al. [26]. Copyright 2015, Royal Society of Chemistry. Reprinted with permission.

photocatalyst, which should have several respects. For example, it is relatively inexpensive, physically and chemically stable, and non-toxic. Also, the band alignment in such a photocatalyst (Figure 3) makes the photogenerated holes to be highly oxidising. In addition, photogenerated electrons have reduction potential enough to produce superoxide radical from oxygen [26,29,30]. TiO_2 is the typical material meeting these criteria. Zhang et al. [31] and Hirakawa and Nosaka [32], based on experimental evidence, proved that the conduction band electrons in TiO_2 have the potential to generate superoxide radicals ($O_2^{\cdot-}$) from dissolved oxygen in water.

Challenges with TiO_2 application in water treatment

The most studied phases of TiO_2 are anatase and rutile. The anatase phase is known to display higher photocatalytic activity than the rutile phase. The low activity observed in rutile ($E_g = 3.0$ eV, $\lambda = 413$ nm), despite its lower bandgap energy than anatase ($E_g = 3.2$ eV, $\lambda = 388$ nm), is attributed to the rapid rate of electron–hole recombination. Also, the CBM of anatase is about 0.2 eV higher than that of rutile (Figure 3). This implies that the conduction band electrons in anatase are more reductive than those in rutile [33,34]. However, the inefficient utilisation of visible light and high recombination rate of photoelectrons and holes, that drastically reduces quantum efficiency, are the major drawbacks of photocatalytic application [28,35]. The challenges with TiO_2 as a potential photocatalyst for the removal of organic pollutants in wastewater are summarised in Figure 4.

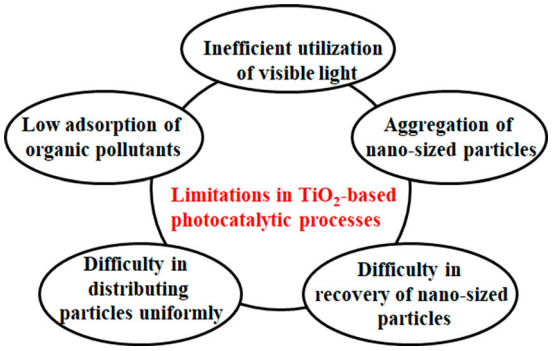

Figure 4 Limitations in TiO_2-based photocatalytic processes for the degradation of organic pollutants. Adapted from Dong et al. [34]. Copyright 2015, Elsevier. Reprinted with permission.

Visible light activity

The ultraviolet (UV) region only accounts for <5% of the entire solar spectrum, which TiO_2 is responsive to. The strategies used in extending the optical absorption of TiO_2 into the visible region include, metal-doping, non-metal doping, dyes sensitisation and direct reduction of TiO_2 (e.g. hydrogenation, chemical reduction and electrochemical reduction). Three of the methods will be addressed here.

(a) **Metal-doped TiO_2** (e.g. Ag, Pt, Au, Fe, Cu, Co, Ni, Cr, Mn and Ru). This method has been extensively investigated over the past decades for improving the photocatalytic degradation efficiency of TiO_2 for several organic pollutants under visible light ($\lambda > 420$ nm) [34,36]. Ag-doped TiO_2 and Cu-doped TiO_2 are the most reported in photocatalytic water treatment. The lowest bandgap energy reported in the literature for metal-doped TiO_2 is 1.6 eV with 7.5% Cu-doped TiO_2, prepared using a low-temperature hydrolysis reaction [37]. Khan

et al. reported the synthesis of Ag-doped TiO_2 using sol–gel method and the application in photocatalytic degradation of oxytetracycline under UV–visible light irradiation. The experimental results indicated 70% and 100% photocatalytic degradation of oxytetracycline in 60 min with pure TiO_2 and 1.9 wt.% Ag/TiO_2, respectively, under UV–visible light irradiation. With only visible light irradiation ($\lambda > 420$ nm), the degradation efficiency of the 1.9 wt.% Ag/TiO_2 sample reduced drastically to 60% [38]. Generally, for metal-doped TiO_2, the metal ion doping can either be substitutional or interstitial in the TiO_2 crystal lattice and can also form a mixture of oxides [38–43]. The limiting factors with this strategy include the nature of dopant species, dopant concentration, photochemical stability and thermal treatment. Several methods employed in metal-doped TiO_2 (e.g. impregnation, co-precipitation, sol–gel, hydrothermal, spray pyrolysis, ion-assisted sputtering and chemical vapour deposition) were reported [36,44–47]. However, sol–gel method is commonly used in the preparation of nano-size-doped TiO_2 materials. The procedure is simple to carry out and does not require complicated facility [36]. The dopant dosage and calcination temperature play a significant role in photocatalytic activity of prepared TiO_2 samples [48]. The visible light activity of metal-doped TiO_2 is primarily due to the introduction of new energy levels in the bandgap of TiO_2, and photogenerated electrons can be excited from the defect state to the conduction band in TiO_2. Dopant ions above the optimum dosage could act as electron–hole recombination centres and will automatically reduce photocatalytic and quantum efficiencies [34].

(b) **Non-metal-doped TiO_2** (e.g. S, N, C, P, F and B). This method extends the visible light absorption of TiO_2 more than metal-doped counterparts. This is because their impurity states are close to the valence band edge of TiO_2 [34]. Compared to other non-metals, the N-doped and C-doped TiO_2 powders have been reported to show exceptional photocatalytic activity under visible light irradiation. Chen et al. [49] prepared C–TiO_2, N–TiO_2 and C–N–TiO_2 using sol–gel method and tested their photocatalytic activities for the degradation of methylene under visible light irradiation. In the absence of catalysts, about 5% photodegradation of methylene blue was observed in 7 h. The C–N co-doped sample exhibited the highest efficiency with about 95% methylene blue removal in 7 h, while 26, 60 and 70% degradation efficiencies were observed for unmodified TiO_2, N-TiO_2 and C-TiO_2 samples, respectively. Co-doped TiO_2 generally exhibit higher visible light absorption than single-doped TiO_2 due to a synergistic effect between the two dopants, which increases charge carrier lifetime (quantum efficiency) [48]. The major drawbacks associated with non-metal doping include the formation of oxygen vacancies in the bulk in which the created defects act as electron–hole recombination sites, thus reducing the visible light photocatalytic efficiency. More so, instability is a major concern due to liberation of doped non-metals atoms in solution during photocatalysis [50,51].

(c) **Reduced TiO_2** (TiO_{2-x}). Hydrogenation of TiO_2 was reported in 2011 by Chen et al. as an effective method in shifting the bandgap of TiO_2 to around 1.5 eV (~820 nm) with an optical onset of around 1.0 eV (black TiO_2) [52]. The photocatalytic activity of the coloured TiO_2 was compared with unmodified TiO_2 for methylene blue decomposition under solar light irradiation. Complete bleaching of methylene blue was achieved after 8 min for the black TiO_2, while the unmodified white TiO_2 under the same experimental conditions, took nearly 1 h. Under similar experimental conditions, complete degradation of phenol was achieved after 40 min for the black TiO_2, while the unmodified TiO_2 took 80 min to achieve the same. Total organic carbon (TOC) removal efficiency of the black TiO_2 was not reported by the author. Furthermore, without any form of treatment, the black TiO_2 was highly stable after eight successive photocatalytic degradation cycles. This discovery led to an extensive research into coloured TiO_2 synthesis globally. Other methods used in fabricating reduced TiO_2 include Al reduction [53], Zn reduction [54], imidazole reduction [55], $NaBH_4$ reduction [56], CaH_2 reduction [57] and electrochemical reduction [58]. It has been widely accepted that heating TiO_2 under vacuum or in a reducing atmosphere also leads to colour changes [59]. The coloured TiO_2 (red, yellow, blue or black) resulted from the creation of Ti^{3+} or/and oxygen vacancies in the white TiO_2. However, their activities in the visible region are still far from satisfactory [59,60].

Dispersibility

TiO_2 particles suffer from severe aggregation during photocatalytic application, which will reduce their active sites and light-harvesting capability. Since photocatalytic degradation occurs at the surface of TiO_2, mass transfer limitations need to be reduced for its effective application in water treatment [61,62]. Two possible approaches employed are:

(a) **Stabilisation by support structures** (glass beads, fibre glass, glass pellets, glass sheets, silica, organo-clays, stainless steel, Al_2O_3 fibre, quartz

beads, polymers, activated carbon and zeolites) [61]. However, there is still no ideal support that is suitable in terms of mechanical stability and selectivity [62]. Immobilisation on supports reduces TiO_2 surface area-to-volume ratio and the photocatalytic efficiency compared to unsupported TiO_2 particles [63].

(b) **Stabilisation by surface modification** (humic acid, carboxylic acids, amino acids and polylactic acid). This method tends to generate high negatively charged density (zeta potential) on the TiO_2 surface and promotes repulsive forces among particles, thus reduces aggregation rate. The main drawback is the stability of these organic modifiers during photocatalysis [64–67].

Separability

Recovery of fine particles of TiO_2 from solution is a huge challenge in suspension systems. Thus, the recovery and reusability of TiO_2 is required before the technology can proceed beyond lab scale to industrial application. Two potential approaches applied are:

(a) **Immobilisation on solid supports** (glass fibres, glass, quartz and stainless steel). This method has been discussed under TiO_2 particles stabilisation using solid supports [63]. Although this approach overcomes the solid–liquid separation problem, slurry-type reactors are still more efficient over immobilised catalyst-type reactors, due to the availability of catalyst's surface and superior mass transfer properties [68].

(b) **Magnetic separation** (Fe_3O_4, γ-Fe_2O_3, $NiFe_2O_4$, $CoFe_2O_4$, FeCo and Co_3O_4). Compared to other magnetic materials, magnetite (Fe_3O_4) has received considerable attention due to its remarkable magnetic properties, low toxicity and biocompatibility [69–71]. This approach is very convenient for separating, recovering and reusing the fine magnetic TiO_2 particles by applying an external magnetic field [72,73]. It was reported that a direct deposition of TiO_2 onto the surface of magnetic oxide particles led to severe photo-dissolution of the magnetic core. In order to overcome the challenge, the addition of silica (SiO_2) layer between the magnetic core and the TiO_2 shell provided magnetic nanoparticles with a chemically inert surface, which inhibited the oxidation of the magnetic core (Fe_3O_4) by the photogenerated VB holes in the outer layer (TiO_2) [74]. The synthesis of a multipurpose catalyst (graphene/TiO_2/SiO_2/Fe_3O_4) was reported for the degradation of 2,4-dichlorophenoxyacetic acid (a herbicide). It took the advantages of TiO_2 photocatalysis, graphene (excellent electron transfer ability and high adsorption capability), Fe_3O_4 (magnetic separation) and SiO_2 (suppressing photo-dissolution of the magnetic core). The TiO_2 composite achieved 100% degradation of 2,4-D under simulated solar irradiation, while commercial P25 recorded only 33% under the same conditions. More so, the composite was highly stable after eight successive cycles. The photocatalytic activity was dependent on the calcination temperature, magnetic core size and the silica layer content [75,76].

Adsorption capacity

The photocatalytic activity of TiO_2 is also dependent on its adsorption capacity for the pollutants in aqueous solution. Several approaches have been used to overcome the low adsorption capacity of TiO_2. Modification of TiO_2 with some chelating ligands (arginine and salicylic acid) and carbon nanomaterials (graphene, carbon nanotubes and activated carbon) have been reported to enhance the adsorption of organic water contaminants [77–79]. With respect to doping with carbon-based nanoparticles, the higher adsorption capability and better photocatalytic activity were reported to be related to their high surface area, high conductivity and high visible light absorption intensity [54,55].

Photocatalytic degradation of chlorophenols

Various studies show that the rate of degradation of CPs is dependent on, solution pH [80–84] and molecular structure – especially the number of substituted Cl groups and their positions on the benzene ring relative to the hydroxyl group [85–87]. It is well known that the initial degradation rate of most organic pollutants with TiO_2 and other photocatalysts follows the pseudo-first-order reaction model [85,88–91]. Table 2 summarises the recent findings (mainly over the past five years) on the application of TiO_2-based photocatalysts for the photocatalytic degradation of CPs in aqueous solution.

Yu et al. prepared a magnetically separable TiO_2/FeO_x microstructure decorated with poly-oxo-tungstate (POM) using hydrothermal method. The photocatalytic degradation of an endocrine disruptor 2,4-dichlorophenol (2,4-DCP) was evaluated under low-intensity solar light [92]. Non-magnetic TiO_2/POM (1%) led to the fastest 2,4-DCP degradation kinetics with 87.6%, compared to magnetically separable TiO_2/FeO_x (25%)/POM(1%) and bare TiO_2 with 76% and 50% 2,4-DCP degradation in 180 min,

Table 2. Progress on TiO_2 photocatalysis for the degradation of chlorophenols over the past five years.

TiO_2-based photocatalysts	Bandgap energy (eV)	Experimental condition	Performance	Ref.
0.21 mol % Cu–TiO_2 (sol–gel)	Nil	(5 × 7 W) Vis LED (λ = 440–490 nm), catalyst dose (3.0 g L^{-1}), 2-CP concentration (20 ppm, pH = 5.5)	100% degradation in 6 h	[83]
1 wt.% M–TiO_2 (M = Fe, Cu, Ni)	2.5–3.4	(4 × 15 W) UV lamp (λ = 365 nm), cat dose (2.0 g L^{-1}), 4-CP (10 ppm)	Ni (90%, 80%), Cu (90%, 73%), Fe (37%, 31%) degradation and TOC removal, respectively, in 6 h	[88]
Magnetic TiO_2/FeO_x/POM	2.65	Simulated solar light, cat dose (0.5 g L^{-1}), 2,4-DCP conc (10 mg L^{-1}, pH = 5)	76% degradation and 55.9% TOC removal in 180 min	[92]
Fe_3O_4/SiO_2/La-TiO_2 (sol–gel)	nil	UV–visible light (λ > 340 nm), catalyst dose (2.0 g L^{-1}), TCP conc (10 μM)	90% degradation in 60 min	[93]
V_2O_5/TiO_2/CTAB (solid-state dispersion)	2.21	64-W UV-B lamp, catalyst dose (2 g L^{-1}), DCP (25 mg L^{-1}, pH = 5)	100% degradation in 30 min, 97% TOC removal	[94]
C/Cl–TiO_2@C_3N_4 NTs	nil	300 W Xe lamp (λ > 420 nm), catalyst dose (1.0 g L^{-1}), PCP conc (20 mg L^{-1})	100% degradation in 4 h, 75% TOC removal in 18 h	[95]
TiO_2 (P25)	3.1	500 W Xe lamp (λ > 365 nm), catalyst dose (0.02 g L^{-1}), PCP conc (10 μM)	~90% degradation in 15 min	[96]
Ag/TiO_2 (photodeposition)	Nil	40 W UV LED (λ = 365 nm), catalyst dose (1.0 g L^{-1}), 4-CP conc (10 ppm)	90% degradation in 60 min, 25% TOC removal in 60 min	[97]
TiO_2–RGO–CoO (sol–gel)	2.83	200 W Xe lamp (visible light), catalyst dose (0.5 g L^{-1}), 2-CP conc (10 mg L^{-1}, pH = 6)	98.2% degradation in 8 h	[98]
N–In–Sn–TiO_2 (sol–gel)	3.10	UV and vis light (λ > 400 nm), cat dose (0.125 and 0.25 g L^{-1}), 4-CP conc (50 μM, pH = 5.38)	96% degradation in 1 h (UV), 90.7% degradation in 8 h (Vis)	[99]
8.0 wt.% B-TiO_2 (sol–gel)	2.89	(18 × 8 W) UV-A lamp and (2 × 150 W) visible light (λ > 400 nm), catalyst dose (1.0 g L^{-1}), 2,4-DCP (20 mg L^{-1}, pH = 6.5)	90% degradation in 5 h (UV), 75% degradation in 5 h (Vis)	[100]
I/TiO_2 –T (5/2) *n*(Ti)/*n*(I) ratio of 5/2 (lignin as template, T)	3.16	350 W Xe lamp (λ > 400 nm), catalyst dose (0.5 g L^{-1}), 4-CP concentration (50 mg L^{-1})	100% degradation in 60 min, ~90% TOC removal in 100 min	[101]
CdS@TiO_2	2.25	Mic-LED-455 (visible light), cat dose (1.0 g L^{-1}), CPs (10 mg L^{-1})	73.8% (2,4-DCP) and 77% (2,4,6-TCP) degradation in 360 min	[102]
Fe_3O_4@TiO_2@Au	nil	150 W Xe lamp (UV–vis light), cat dose (0.5 g L^{-1}), TCP conc (7.5×10^{-5} M, pH = 10)	97.7% degradation in 40 min	[103]
2 wt.% CuS/TiO_2	2.73	125 W Hg lamp (λ = 365 nm), 4-CP (20 mg L^{-1}, 60 mL)	87% degradation in 150 min	[104]
M/TiO_2 (M = CoPc or ZnPc)	2.67–2.78	128 W Lightex LT50 lamp (visible light), cat dose (1.0 g L^{-1}), 4-CP (0.013 M, pH = 7)	99% degradation in 30 min (with both samples)	[105]
Y_2O_3/TiO_2 nanosheets	2.92–3.20	Natural sunlight, cat dose (1.0 g L^{-1}), 4-CP (20 mg L^{-1})	98% degradation and 67.6% TOC removal in 120 min	[106]
7 wt.% (Fe_2O_3, Co_3O_4 and CuO) loaded $ZnTiO_3$–TiO_2	2.82–3.12	Natural sunlight, 0.3 mL H_2O_2, cat dose (2.0 g L^{-1}), 4-CP conc (25 mg L^{-1}, pH = 5)	100%, 76% and 85% degradation in 45 min with Fe_2O_3, Co_3O_4 and CuO, respectively	[107]
Fe–TiO_2–Ag nano-sphere (0.3 wt.% Fe and 2.0 wt.% Ag)	nil	(2 × 8 W) UV-C lamp, cat dose (1.5 g L^{-1}), 4-CP conc (40.4 mg L^{-1}, pH = 4.86)	97% degradation in 165 min	[108]
10 wt.% GO–TiO_2 (titanate nanotubes)	2.8	UV lamp (λ = 254 nm), cat dose (1.0 g L^{-1}), 4-CP conc (50 ppm)	65% degradation in 175 min	[109]
FeOOH/TiO_2 (0.14 wt.% Fe)	3.1	300 W Xe lamp (λ > 320 nm), cat dose (0.5 g L^{-1}), 2,4,6-TCP conc (50 mg L^{-1})	100% degradation and 85% TOC removal in 240 min	[110]

CTAB, cetyl trimethylammonium bromide; NTs, nanotubes; RGO, reduced graphene oxide; Pc, phthalocyanine; GO, graphene oxide; POM, poly-oxo-tungstate.

respectively, under simulated solar light at pH 5.0. POM was reported to scavenge electrons from the conduction band of TiO_2 to decrease the charge recombination, thus enhancing the photocatalytic (quantum) efficiency of TiO_2. Peng et al. synthesised a multipurpose photocatalyst, La-doped magnetic TiO_2 ($Fe_3O_4/SiO_2/La\text{-}TiO_2$) using sol–gel method and investigated its photocatalytic activity for 2,4,6-TCP degradation [93]. The magnetic $La\text{-}TiO_2$ exhibited a higher photocatalytic degradation activity (90% in 60 min) compared to magnetic TiO_2 (50%). However, the La-doped magnetic TiO_2 was fairly stable after seven successive cycles. The drawback was attributed to the reduction in surface hydroxyl groups and reaction sites on TiO_2.

Sinirtas et al. [94] prepared a binary oxide catalyst (V_2O_5/TiO_2) using solid-state dispersion method and evaluated the photocatalytic activity for 2,4-dichlorophenol degradation under UV–visible light irradiation. Photocatalytic degradation efficiencies of 55%, 60%, 70% and 85% were achieved in 30 min with TiO_2 (synthesised), commercial TiO_2 (P25), V_2O_5 and V_2O_5/TIO_2, respectively. The effect of surfactant additives (CTAB, HTAB and PVA) on the photocatalytic activity of the binary oxide catalyst was also investigated. Under similar operating conditions, the (V_2O_5/TiO_2/CTAB) sample displayed the highest activity (complete degradation in 30 min), while the samples prepared with HTAB and PVA recorded degradation efficiencies of ~92% and ~55%, respectively. The enhanced photocatalytic performance of V_2O_5/TiO_2/CTAB was attributed to an appropriate pore distribution and high separation efficiency of photoinduced charge carriers. However, the photochemical stability of V_2O_5/TiO_2/CTAB was not reported.

Photocatalytic reduction of heavy metals

Hexavalent chromium

The discharge of hexavalent chromium (Cr(VI)) from industrial processes, such as electroplating, leather tanning, metal fabrication, paint and pigment production into the aquatic environment has raised serious concerns over the potential water pollution issues [111,112]. In this regard, the reduction of toxic and carcinogenic Cr(VI) to the less harmful Cr (III) is imperative to mitigate their adverse effects towards biological and environmental systems. Over the years, photocatalytic reduction of Cr(VI) by TiO_2 photocatalysts has been regarded as one of the more promising treatment alternatives owing to its direct one-step photocatalytic reduction of Cr(VI) under UV light irradiation [113–115]. Table 3 summarises the recent findings (mainly over the past five years) on the application of TiO_2-based photocatalysts for the photocatalytic reduction of aqueous-based Cr (VI).

The simplified mechanism for the photocatalytic reduction process: $Cr_2O_7^{2-} + 14H^+ + 6e^- \rightarrow 2Cr^{3+} + 7H_2O$, indicating that the photogenerated electrons separated from the electron–hole pairs are solely responsible for the photocatalytic reduction of Cr (VI) to Cr(III). Lin et al. [131] revealed that the initial reduction rate of Cr(VI) using TiO_2 photocatalyst is following the Langmuir reaction model. They also discussed on the pH-related thermodynamic aspects of the photocatalytic reduction of Cr(VI), as well as found that the photocorrosion of TiO_2 to be relatively unfavourable in basic media. Ku and Jung [132] evaluated the photocatalytic reduction rates of Cr(VI) under various operating conditions (i.e. solution pH, initial Cr(VI) concentration, TiO_2 photocatalyst loads, light intensities and the presence of scavengers). They found a higher photocatalytic reduction rate of Cr(VI) in acidic medium than in basic medium, which is contradicting to the previous study by Lin et al. [131]. The higher photocatalytic reduction rate of Cr(VI) in acidic medium is attributed to the highly positively charged TiO_2 surfaces, as well as the presence of less competing molecules for redox reaction at the lower pH. Yoon et al. [133] immobilised TiO_2 photocatalysts onto inert substrates to overcome the photocatalysts' recovery and post-separation issues via anodising various nanotubular TiO_2 arrays under oxygen stream in the range 450–850°C for reduction of Cr(VI). Their findings demonstrated that anodised nanotubular TiO_2 arrays annealed at 450°C exhibited the highest reduction efficiency of Cr(VI) at 98% along with a hydrogen evolution rate of 38 μmol h^{-1} cm^{-2}. The presence of higher-activity anatase TiO_2 phase in the anodised nanotubular TiO_2 arrays annealed at lower temperatures (<450°C) could explain their excellent reduction efficiency of Cr(VI) [134].

In order to develop highly efficient TiO_2-based photocatalysts with extended absorption into the visible light spectrum, the introduction of dopants into morphological-modified TiO_2-based photocatalysts has been proven as an effective strategy. The introduction of dopants could hinder the rapid recombination rate of electron–hole pairs and narrowing the wide bandgap of TiO_2 photocatalysts and hence, improving its visible light photocatalytic activity. Lu et al. [135] optimised the amount of vanadium (V) dopant on TiO_2 nanosheets since this sheet-like structure possesses higher exposed surface areas for Cr(VI) adsorption. It is noteworthy that the introduction of V dopant resulted in the reduction of TiO_2 bandgap leading to a high visible light photoactivity, and the co-existence of RhB and Cr(VI) greatly improved photocatalytic degradation kinetics as Cr(VI) is an efficient scavenger of photogenerated electrons.

Table 3. Recent studies on TiO_2-based photocatalysts for photocatalytic reduction of Cr (VI).

TiO_2-based photocatalysts	Dopants/cocatalysts	Bandgap energy (eV)	Initial concentration and pH	Light sources	Performance	Ref.
g-C_3N_4/Ti^{3+}-TiO	g-C_3N_4 (6 wt-%)	2.7–3.1	10 mg L^{-1}; pH 2	300 W Dy lamp with a 400 nm cutoff filter	~90% Cr(VI) removal in 120 min	[116]
(C, N and S)-TH–TiO_2	Molar ratio of TH to Ti = 1.5:1 C: 10.24 wt-% N: 0.92 wt-% S: 1.15 wt-%	2.95	10 mg L^{-1}; pH 2	500 W Xe lamp	>99% Cr(VI) removal in 50 min	[117]
nZVI–TiO_2	$FeCl_3{\cdot}6H_2O$ (50 wt-%)	Nil	6 mg L^{-1}; pH 3	18 W UV-C lamp	100% Cr(VI) removal in 2 h	[118]
AgI–TiO_2	AgI (5%)	2.67–2.83	8.3 mg L^{-1}; pH 1	300 W halogen lamp	99% Cr(VI) removal in 10 min	[119]
TiO_2–graphene hydrogel	TiO_2 (20%)	Nil	5 mg L^{-1}; pH 5.5	250 W Hg lamp (λ: 365 nm)	100% Cr(VI) removal within 30 min	[120]
PAN-CNT/TiO_2-NH_2	PAN (10 wt-%)	Nil	20 mg L^{-1}; pH 2	120 W Xe lamp (λ: 420 nm; E_e: 100 mW cm^{-2})	>90% Cr(VI) removal in 30 min	[121]
Cu/Cu_2O/SA/TiO_2 beads	Weight ratio of TiO_2 to SA (1:1); C: 12.83% w/w; H: 2.45% w/w	Cu_2O/TiO_2 = 1.9–2.2	5 mg L^{-1}; pH 4	9 W UV-A lamps (λ: 365 nm); 9 W visible lamps (E_e: 7.2 mW cm^{-2})	100% Cr(VI) removal in 15 min under UV irradiation; >90% Cr(VI) removal in 100 min under visible light irradiation	[122]
rGO-TiO_2	rGO (5 wt-%)	2.82	10 mg L^{-1}; pH 3	Xe lamp (E_e: 300 mW cm^{-2})	98% Cr(VI) removal in 180 min	[123]
Algae-Ag/TiO_2	$AgNO_3$: 0.5%; TiO_2: 1%; weight ratio of chitosan to PVA (1:1)	Nil	5 mg L^{-1}; pH 2	500 W halogen tungsten lamp	~90% Cr(VI) removal in 180 min	[124]
Fe–N–C–TiO_2	Fe/Ti weight ratio = 0.30%	2.75	20 mg L^{-1}; pH 2	500 W Xe lamp	100% Cr(VI) removal in 240 min	[125]
CeO_2–TiO_2	Molar ratio of Ce to Ti = 1:3	2.49	2.78 mg L^{-1}	Visible light	>99.6% Cr(VI) removal in 60 min	[126]
Cu–TiO_2	Cu (1.5 wt-%)	Nil	5 mg L^{-1}; pH 5	6 W black-light blue lamps	>90% Cr(VI) removal in 60 min	[127]
CD–TiO_2	CD (0.75 wt-%)	Nil	10 mg L^{-1}; pH 3	LED light (λ: 365 nm)	100% Cr(VI) removal within 30 min	[128]
Bi–TiO_2	$BiCl_3$: 0.10 M	2.82	40 mg L^{-1}; pH 4.5	32 W visible light fluorescent lamp	53% Cr(VI) removal within 120 min	[129]
Au/Pt–TiO_2	Au (10 wt-%); Pt (10 wt-%)	Nil	5 mg L^{-1}; pH 2.5	UV LED and green LED	100% Cr(VI) removal in 25 min	[130]

TH, thiourea; PAN, polyacrylonitrile; CNT, carbon nanotubes; SA, sodium ascorbate; PVA, polyvinyl alcohol; CD, carbon dots.

Besides, the V-doped TiO_2 nanosheets could effectively trap photogenerated electrons and introduce a higher density defect (Ti^{3+}), which are essential to enhance the effective separation of photogenerated charge carriers and high quantum efficiency. They extended their works in another study by synthesising TiO_2 nanosheets loaded with Mn_xO_y and CoO_x nanoparticles for simultaneous photocatalytic reduction of Cr(VI) and decontamination of organic compounds [136,137]. Similarly, the introduction of Mn_xO_y and CoO_x nanoparticles resulted in a considerable enhancement of visible-light photoactivity, formation of active electron centres and the generation of Ti^{3+} density defects.

Recently, Xue et al. [138] reported the rational design of an interfacial heterojunction photocatalyst between 2D BiOBr nanoplates and 1D rutile TiO_2 nanorods. Figure 5(a) shows the synthesis route of the heterojunction photocatalyst in which the 1D TiO_2 nanorods are first fabricated using the molten salt flux method followed by the bonding between positively charged alkoxide complexes, Bi-$(OCH_2CH_2OH)^{2+}$ and negatively charged TiO_2 nanorods via solvothermal reaction. This eventually leads to the nucleation of BiOBr nanoplates, which are later being vertically embedded with TiO_2 nanorods to synthesise the heterojunction photocatalyst (i.e. Figure 5 (b)). The HRTEM image (Figure 5(c)) showed the interplanar spacings of 0.230 and 0.248 nm are well corresponded to the {200} and {101} facets of the rutile phase of TiO_2, respectively. While the measured 0.277 and 0.353 nm fringes of BiOBr nanoplates can be assigned to the {110} and {101} planes of tetragonal BiOBr, respectively. Additionally, the rectangular spotty electron diffraction pattern can be clearly observed in Figure 5(d), indicating the single-crystalline rutile phase TiO_2 in this heterojunction photocatalyst. More importantly, the photocatalytic results (Figure 5(e)) indicated that the TB-2 (i.e. the sample with a molar ratio of Ti to Bi, n(Ti/Bi) = 2:1) exhibited the highest photoreduction rate of Cr(VI) with an apparent rate constant of 0.025 min^{-1} under visible light illumination. This is ascribed to the formation of an interfacial junction between BiOBr and TiO_2, which provides directional transfer nanochannels for the migration of photoinduced charge carriers and thus, enhancing quantum efficiency and reducing the charge recombination as evidenced by the PL spectra

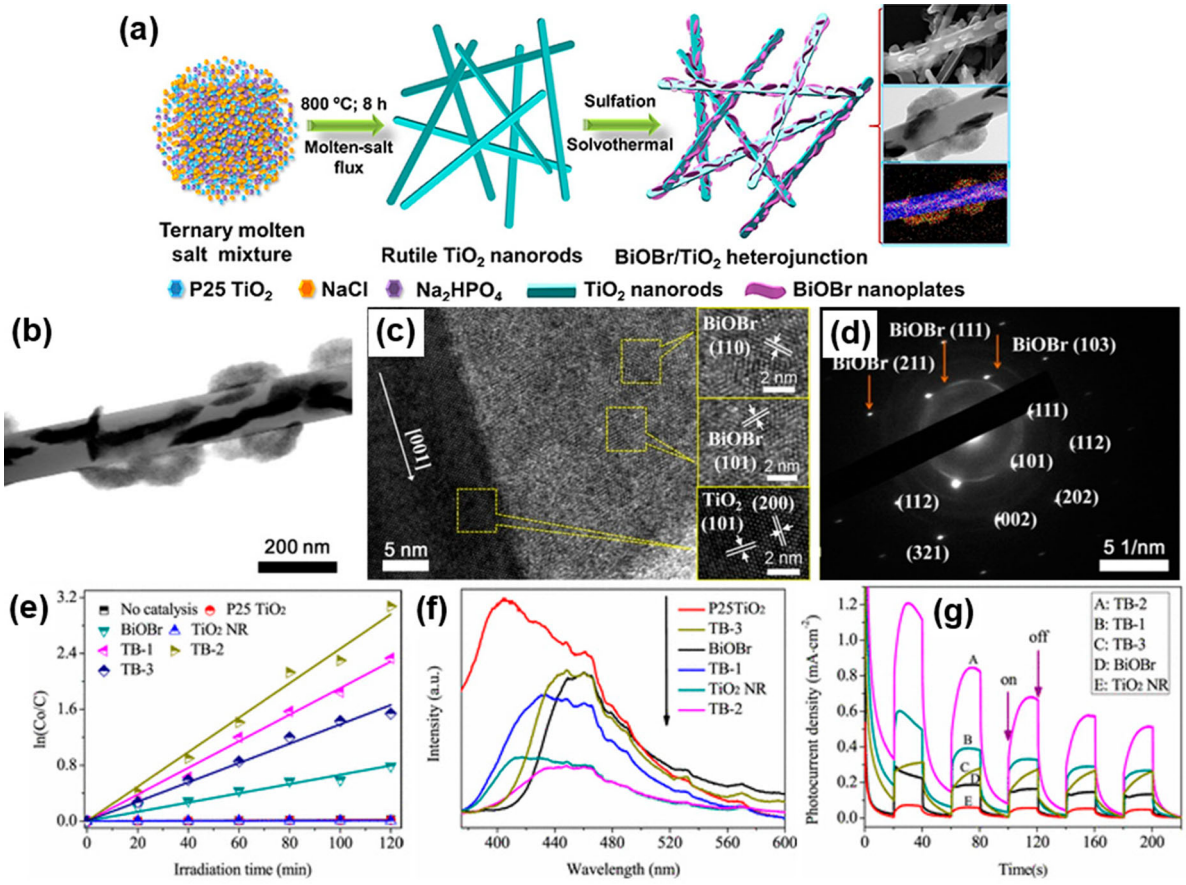

Figure 5. (a) Schematic illustration for the synthesis route of BiOBr nanoplates/TiO_2 nanorods heterojunctions; (b) TEM image; (c) HRTEM image; (d) SAED image of an individual BiOBr/TiO_2 sample; (e) reaction kinetics for photocatalytic reduction of aqueous Cr (VI) over different samples under visible light illumination; (f) PL spectra with an excitation wavelength of 325 nm and (g) transient photocurrent responses under visible light irradiation for all samples. Adapted from Xue et al. [138]. Copyright 2017, American Chemical Society. Reprinted with permission.

in Figure 5(f) leading to highphotoactivity as per Figure 5(g). Interestingly, similar theory on enhanced physisorption and charge transfer of PANI/MnO_2/TiO_2 nanocomposite shows the importance of TiO_2 heterojunctions to improve the visible light-driven photoreduction of Cr(IV) [139].

Pentavalent arsenic

Owing to their carcinogenicity and mutagenicity nature, arsenic (As) compounds contamination in natural water can present a major threat to the environmental system and public health even in a very low concentration [140–142]. Previous studies are mainly focusing on the oxidation of acutely toxic arsenite (As(III)) to arsenate (As(V)); however, the high adsorbability of As(V) on soil could adversely influence bacteria and microscopic fungi [143,144]. Particularly, this section presents the recent findings on the photocatalytic reduction of aqueous As(V) by using TiO_2-based photocatalysts in detail. Previously, Levy et al. [145] have applied pristine TiO_2 photocatalyst to investigate its photoreduction performance over As(V) under UV light in deoxygenated aqueous suspension. They found that the direct reduction of As(V) to As(IV) by accepting photogenerated electrons at conduction band was not thermodynamically possible. Nevertheless, the addition of sacrificial electron donors (i.e. alcohols or carboxylic acids) in the photocatalytic medium could lead to the production of strongly reductive radicals and thus, promoting the indirect reductive mechanism of As(V).

Similarly, the deposition of transition and precious metals onto TiO_2-based photocatalysts has been widely attempted in order to extend their light absorption into the visible light spectrum as well as serving as active centres to inhibit the recombination of electron–hole pairs [34,146]. For instance, Andjelkovic et al. [147] prepared a Fe-doped TiO_2 photocatalyst via microwave-assisted hydrothermal method in order to provide large capacity for the adsorption and removal of As(V). They found that the adsorption efficiency of As(V) was proportional to the amount of Fe(III) dopants because it tends to provide a higher specific surface area which directly responsible for faster As(V) adsorption rate. Isotherm studies showed that the Langmuir model provides the best fitting for the adsorption data of As(V) better and the Fe-doped TiO_2 photocatalyst attained the maximum adsorption capacity of 17.35 mg g^{-1} As(V). In another study, Liu et al. [148] deposited Fe onto morphological-modified titanate nanotubes (TNTs) for sequential As(III) oxidation and As(V) adsorption. The resultant Fe-TNTs exhibited a good adsorption performance for As(V) at acidic medium (i.e. adsorption capacity of ~49.1 mg g^{-1} at pH 3; removal efficiency of 98.2%) due to the opposite surface charges between Fe-TNTs and As(V) anions. It was found that there are two different forms of deposited Fe that could improve the photocatalytic activity through: (1) Fe^{3+} ions that locate in the interlayers to act as temporary electron- or hole-trapping sites, and (2) attached α-Fe_2O_3 that facilitates the charge separation from TNTs to reduce recombination of electron–hole pairs.

A more recent study by Gao et al. investigated the performance of a 3D cake-like COOH functionalised anatase (TiO_2@C) (Figure 6(a,b)) for simultaneous Cr(VI) reduction and As(III) oxidisation followed by the adsorption of As(V) [149]. The simultaneous conversion of Cr(VI) and As(III) was significantly enhanced from 14.5% to 61.8% and 38.5% to 92%, respectively, in the exposure system of TiO_2@C/As (III)/Cr(VI). It is worth mentioning that As(V), which was oxidised from As (III), has also been effectively removed under acidic condition, as shown in Figure 6(c). Moreover, they also reported that the removal rate of As(V) was essentially relied upon the pH, TiO_2@C dosage (Figure 6(d)) and initial concentration of Cr(VI)/As(III) solution (Figure 6(e)). Before the reaction, Figure 6(f) shows the full XPS spectrum of TiO_2@C containing carbon groups, oxygen and titanium elements. The characteristic peaks of As (III) (45.1 eV) and As(V) (46.1 eV) were detected on TiO_2@C with the proportion of 48.5% and 51.5%, respectively, after exposure to Cr(VI)/As(III) solution (Figure 6(g)) [150]. As a result, the removal performance of As(III)/Cr(VI) using TiO_2@C was improved through co-adsorption of As(III) and Cr(VI) ions, accelerated electrons transfer from As(III) to Cr(VI) initiated by carboxyl groups on TiO_2, and larger binding sites provided by TiO_2 surface.

Outlook

After decade's development on different photocatalysts, TiO_2 is still widely recognized as the best semiconductor material for real application in photocatalytic water purification technology due to its low toxicity, high stability and availability. However, TiO_2 is confronted with some limiting factors such as poor visible light absorption, low photonic efficiency and low adsorption capacity. In this review, we have highlighted various strategies for TiO_2 modification (such as ion doping, cocatalyst decoration and heterojunction formation) not only to improve its light absorption but also to enhance charge separation. Furthermore, this review summarises the recent application of TiO_2-based photocatalysts for the catalytic oxidation of CPs and reduction of heavy metal ions such as chromium and arsenic in aqueous solution, which are two typical while the most challenging topics.

The co-doping of TiO_2 with a metal and non-metal is receiving considerable attention and proved to be

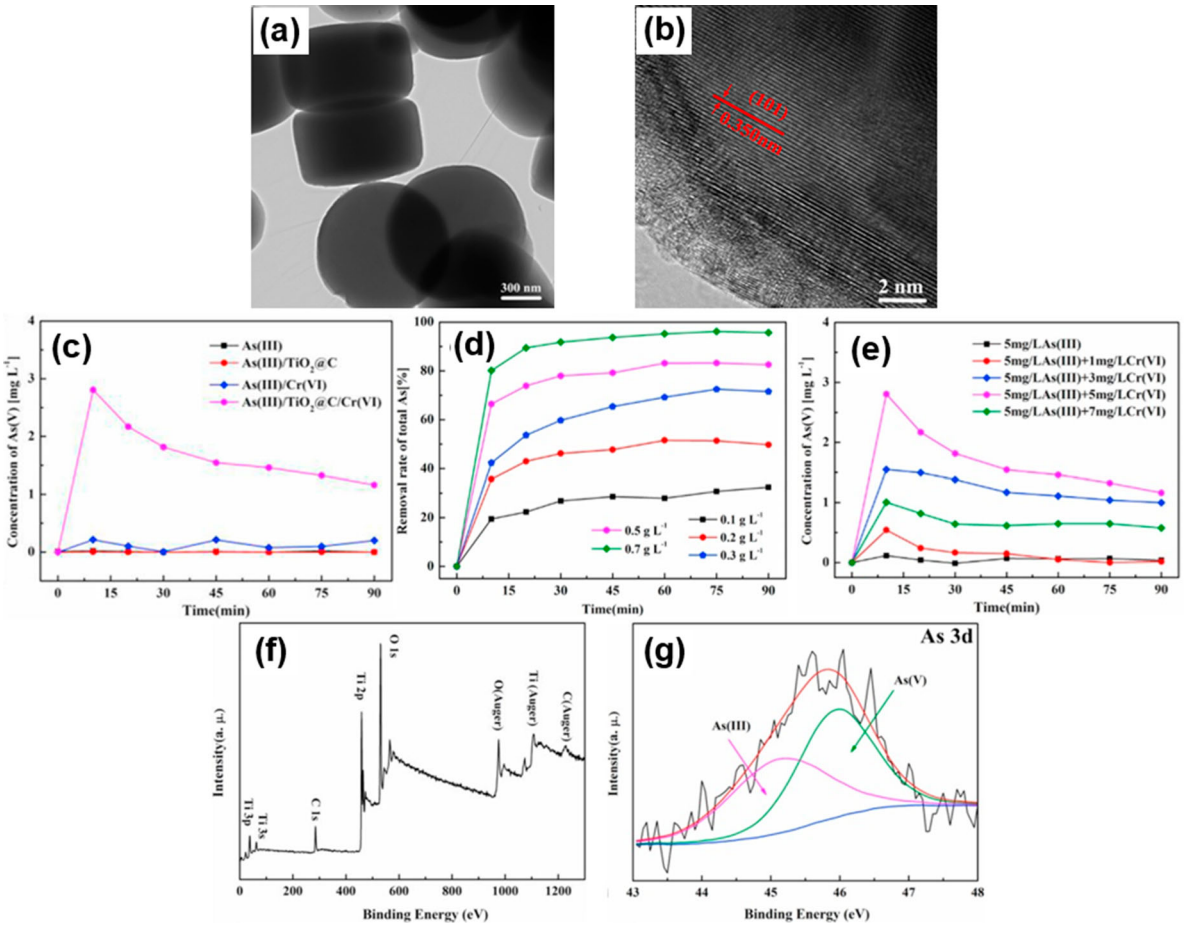

Figure 6. (a) TEM and (b) HRTEM images of TiO_2@C; (c) As(V) production in various solution (As(III) concentration: 6.5 mg L^{-1}; Cr (VI) concentration: 5.5 mg L^{-1}; TiO_2@C concentration: 0.3 g L^{-1}; pH: 3.0; time: 90 min); (d) effect of TiO_2@C dosage on removal of total As (As(III) concentration: 5 mg L^{-1}; Cr(VI) concentration: 5 mg L^{-1}; TiO_2@C concentration: 0.1, 0.2, 0.3, 0.5, 0.7 g L^{-1}; time: 90 min; *T*: 20 ± 2°C pH: 3.0); (e) effect of Cr(VI) initial concentration on adsorption of As(V) (As(III) concentration: 6.5 mg L^{-1}; Cr (VI) concentration: 0–7 mg L^{-1}; TiO_2@C concentration: 0.3 g L^{-1}; time: 90 min; *T*: 20 ± 2°C pH: 3.0); XPS spectra of (f) pure TiO_2@C full spectrum before reaction; and (g) As 3d spectra of TiO_2@C after exposed in As(III)/Cr(VI) solution. Adapted from Gao et al. [149]. Copyright 2018, Elsevier. Reprinted with permission.

more effective than single ion doping towards efficient photocatalytic degradation of organic contaminants in water. This improvement was attributed to an extension in the visible light absorption capacity. Apart from the suppression of photogenerated electron–hole recombination rate, the bandgap energy is also largely decreased due to the introduction of impurity energy levels above the valence band and below the conduction band. The solution pH is also an important operating variable in photocatalytic degradation of organic contaminants. In most TiO_2-based studies, it was shown that acidic pH range (4–6) is the optimum for the efficient degradation of organic substrates in water. This was attributed to the positively charged surface of TiO_2, favouring increased adsorption capacity for organic compounds. It is also worth noting that the fabrication of different bandgap alignments (i.e. Type I, II and III) and Z-scheme heterojunctions was proved to efficiently enhance charge separation of photogenerated electron–hole pairs and reduce the charge carriers recombination rate, beneficial to photocatalytic water treatment.

Reduction of a reactive, high oxidation state of metal ion to a lower oxidation state and less toxic species by TiO_2-based photocatalysts has been regarded as an effective approach for heavy metal removal from aqueous environment. Upon UV light irradiation, the anodic and cathodic redox reactions are initiated, whereby the water oxidation by photoholes is involved and thus transfer of photoexcited electrons from the conduction band of TiO_2 photocatalysts to the adsorbed heavy metal ions takes place. Acceptance of electrons into the metal atom (reduction) could suppress its reactivity and thus, the toxicity effect. Additionally, it is also showed that the equilibrium adsorption capacity of TiO_2 photocatalysts is higher at lower pH medium, signifying a higher density of adsorption sites for heavy metals. In order to extend the functionality and applicability of TiO_2 photocatalysts in visible light range, several material modification strategies such as morphological alteration, dopants introduction and heterojunction are proved to be effective to separate the photogenerated charge carriers and

therefore, leveraging the photon responsiveness of pristine TiO_2 photocatalysts.

For both photocatalytic organic contaminants decomposition and heavy metal ions reduction, cocatalysts play a proved key role, which not only help charge separation but also lower the reaction barrier. The so far best cocatalyst is still noble metal, e.g. Pt. To develop a low-cost cocatalsyt is also important for TiO_2 photocatalyst application. Based on the above discussion, we proposed that the future commercial and large-scale application of photocatalysis in water treatment is feasible if the following could be solved:

- The preparation of low cost, reproducible and environmental-friendly cocatalyst/TiO_2-based photocatalysts that can be photo-activated by solar light (not artificial UV light).
- The efficient recovery and reuse of the photocatalysts during water purification via immobilisation on flexible and highly stable support materials.
- The design of photocatalyst materials capable of selective photocatalytic oxidation of organic pollutants or reduction of heavy metal ions in water.
- The design of efficient photocatalytic reactor with satisfactory efficiency in acidic, neutral and basic media, reflecting the real environment of the wastewater.

The fundamental understanding underlying the photochemical process is still far behind discovery of the photocatalysts.

The photocatalytic mechanism of a single photocatalyst is relatively simple and to some extent straightforward. The photochemical reaction involves the excitation of electrons to the conduction band of a photocatalyst while leaving positive holes at the valence band upon light illumination whereby the photon energy ($h\nu$) is greater than or equal to the bandgap energy of photocatalyst. Studies on charge carrier dynamics have been successfully investigated over the years using time-resolved analytical techniques (time-resolved absorption spectroscopies) to observe the generation, trapping, and transfer of electrons and holes during photocatalytic processes [151,152]. The generation of hydroxyl radicals and superoxide radicals in aqueous systems have been widely established in the literature through spin trapping ESR experiments and fluorescence spectroscopy. The next step is still unclear. The discovery of hydrogen peroxide in oxygen-free systems justifies the generation of hydroxyl radicals by valence band holes, though hydrogen peroxide can also be generated through oxygen reduction. It is still difficult to distinguish the hydroxyl radicals generated from both different pathways, that is, hole oxidation of adsorbed water/hydroxyl ions or through oxygen reduction. Different hydroxyl radical production pathway will provide a different route for improvement of the photocatalytic activity. More importantly, although the time-resolved IR has been successfully employed to other fields, e.g. homogeneous photocatalysis, it has not been used in water treatment. By using this cutting edge technology, the detailed reaction pathway and the rate-determining step could be elucidated, which can also indicate the factor to mitigate the toxic byproducts production during photocatalytic contaminants' treatment and heavy metal cation reduction. In addition, the development of highly efficient photocatalysts is growing intensively, the photocatalytic mechanism within the complex photocatalyst systems and compositing structures is also important while more challenging. These time-resolved spectroscopies should be applied to these complicate systems to understand the reaction pathway. Overall, a practical photocatalytic system for water treatment still requires substantial efforts.

Acknowledgements

A.S. and J.T. thank the Leverhulme Trust (RPG-2017-122), EPSRC (EP/S018204/2) and Royal Society-Newton Advanced Fellowship grant (NAF\R1\191163). All authors are thankful to the other Royal Society-Newton Advanced Fellowship grant (NA150418).

Disclosure statement

No potential conflict of interest was reported by the authors.

Funding

This work was supported by Engineering and Physical Sciences Research Council: [Grant Number EP/S018204/2]; Leverhulme Trust: [Grant Number RPG-2017-122]; Newton Fund: [Grant Number NAF\R1\191163]; Newton Fund: [Grant Number NA150418].

ORCID

Ayoola Shoneye http://orcid.org/0000-0002-6137-8686
Junwang Tang http://orcid.org/0000-0002-2323-5510

References

[1] Ahmed S, Rasul MG, Martens WN, et al. Heterogeneous photocatalytic degradation of phenols in wastewater: a review on current status and developments. Desalination. 2010;261:3–18. doi:10.1016/j.desal.2010.04.062.
[2] Kolpin DW, Furlong ET, Meyer MT, et al. Pharmaceuticals, hormones, and other organic wastewater contaminants in U.S. streams, 1999–2000 : a national reconnaissance. Environ Sci Technol 2002;36:1202–1211. doi:10.1021/es011055j
[3] Schriks M, Van Leerdam JA, van der Linden SC, et al. High-resolution mass spectrometric identification and quantification of glucocorticoid compounds in

various wastewaters in the Netherlands. Environ Sci Technol. 2010;44:4766–4774. doi:10.1021/es100013x
[4] ATSDR. Comprehensive Environmental Response, Compensation, and Liability Act (CERCLA) priority list of hazardous substances; 2007.
[5] Häggblom MM, Bossert ID. Halogenated organic compounds – a global perspective. Boston (MA): Kluwer Academic Publishers; 2003.
[6] Al-Asheh S, Banat F, Abu-Aitah L. Adsorption of phenol using different types of activated bentonites. Sep Purif Technol. 2003;33:1–10. doi:10.1016/S1383-5866(02)00180-6
[7] Murcia JJ, Hidalgo MC, Navío JA, et al. Study of the phenol photocatalytic degradation over TiO_2 modified by sulfation, fluorination, and platinum nanoparticles photodeposition. Appl Catal B: Environ. 2015;179:305–312. doi:10.1016/j.apcatb.2015.05.040
[8] Yang CF, Lee CM. Pentachlorophenol contaminated groundwater bioremediation using immobilized Sphingomonas cells inoculation in the bioreactor system. J Hazard Mater. 2008;152:159–165. doi:10.1016/j.jhazmat.2007.06.102
[9] Murcia N, Gomez MD, Gomez M, et al. Degradation of 4-chlorophenol using Pseudomonas putida. Chem Eng. 2007;10:2–4.
[10] Diagboya PN, Olu-Owolabi BI, Adebowale KO. Microscale scavenging of pentachlorophenol in water using amine and tripolyphosphate-grafted SBA-15 silica: batch and modeling studies. J Environ Manage. 2014;146:42–49. doi:10.1016/j.jenvman.2014.04.038
[11] Olaniran AO, Igbinosa EO. Chlorophenols and other related derivatives of environmental concern: properties, distribution and microbial degradation processes. Chemosphere. 2011;83:1297–1306. doi:10.1016/j.chemosphere.2011.04.009
[12] ATSDR. Toxicological profile for chlorophenols. US Department of Health and Human Services, Atlanta, GA; 1999.
[13] Czaplicka M. Sources and transformations of chlorophenols in the natural environment. Sci Total Environ. 2004;322:21–39. doi:10.1016/j.scitotenv.2003.09.015
[14] U.S. EPA. Edition of the drinking water standards and health advisories. U.S. EPA, Washington (DC): 2004.
[15] Zangeneh H, Zinatizadeh AAL, Habibi M, et al. Photocatalytic oxidation of organic dyes and pollutants in wastewater using different modified titanium dioxides: a comparative review. J Ind Eng Chem. 2015;26:1–36. doi:10.1016/j.jiec.2014.10.043
[16] Karci A, Arslan-Alaton I, Olmez-Hanci T, et al. Transformation of 2,4-dichlorophenol by H_2O_2/UV-C, Fenton and photo-Fenton processes: oxidation products and toxicity evolution. J Photochem Photobiol A: Chem. 2012;230:65–73. doi:10.1016/j.jphotochem.2012.01.003
[17] Bandara J, Mielczarski JA, Lopez A, et al. 2. Sensitized degradation of chlorophenols on iron oxides induced by visible light. Appl Catal B: Environ. 2001;34:321–333. doi:10.1016/S0926-3373(01)00225-9
[18] López Cisneros R, Gutarra Espinoza A, Litter MI. Photodegradation of an azo dye of the textile industry. Chemosphere. 2002;48:393–399. doi:10.1016/S0045-6535(02)00117-0
[19] Konsowa AH, Ossman ME, Chen Y, et al. Decolorization of industrial wastewater by ozonation followed by adsorption on activated carbon. J Hazard Mater. 2010;176:181–185. doi:10.1016/j.jhazmat.2009.11.010
[20] Venkatachalam N, Palanichamy M, Murugesan V. Sol–gel preparation and characterization of alkaline earth metal doped nano TiO_2: efficient photocatalytic degradation of 4-chlorophenol. J Mol Catal A: Chem. 2007;273:177–185. doi:10.1016/j.molcata.2007.03.077
[21] Ray AK, Beenackers AACM. Novel photocatalytic reactor for water purification. AIChE J. 1998;44:477–483. doi:10.1002/aic.690440224
[22] Moniz SJA, Shevlin SA, An X, et al. Fe_2O_3-TiO_2 nanocomposites for enhanced charge separation and photocatalytic activity. Chem Eur J. 2014;20:15571–15579. doi:10.1002/chem.201403489
[23] Yang L, Yu LE, Ray MB. Photocatalytic oxidation of paracetamol: dominant reactants, intermediates, and reaction mechanisms. Environ Sci Technol. 2009;43:460–465. doi:10.1021/es8020099
[24] Khataee AR, Kasiri MB. Photocatalytic degradation of organic dyes in the presence of nanostructured titanium dioxide: influence of the chemical structure of dyes. J Mol Catal A: Chem. 2010;328:8–26. doi:10.1016/j.molcata.2010.05.023
[25] An X, Liu H, Qu J, et al. Photocatalytic mineralisation of herbicide 2,4,5-trichlorophenoxyacetic acid: enhanced performance by triple junction Cu-TiO_2-Cu_2O and the underlying reaction mechanism. New J Chem 2015;39:314–320. doi:10.1039/C4NJ01317D
[26] Wu W, Jiang C, Roy VAL. Recent progress in magnetic iron oxide – semiconductor composite nanomaterials as promising photocatalysts. Nanoscale. 2015;7:38–58. doi:10.1039/c4nr04244a
[27] Park H, Park Y, Kim W, et al. Surface modification of TiO_2 photocatalyst for environmental applications. J Photochem Photobiol C: Photochem Rev. 2013;15:1–20. doi:10.1016/j.jphotochemrev.2012.10.001
[28] Martin DJ, Liu G, Moniz SJA, et al. Efficient visible driven photocatalyst, silver phosphate: performance, understanding and perspective. Chem Soc Rev. 2015;44:7808–7828. doi:10.1039/C5CS00380F
[29] Vinu R, Madras G. Environmental remediation by photocatalysis. J Indian Inst Sci. 2010;90:189–230.
[30] Saito H, Nosaka Y. Mechanism of singlet oxygen generation in visible-light-induced photocatalysis of gold-nanoparticle-deposited titanium dioxide. J Phys Chem C. 2014;118:15656–15663. doi:10.1021/jp502440f
[31] Zhang X, Chen YL, Liu RS, et al. Plasmonic photocatalysis. Rep Prog Phys. 2013;76:046401, doi:10.1088/0034-4885/76/4/046401
[32] Hirakawa T, Nosaka Y. Properties of $O_2^{\bullet-}$ and $OH^{\bullet}$ formed in TiO_2 aqueous suspensions by photocatalytic reaction and the influence of H_2O_2 and some ions. Langmuir. 2002;18:3247–3254. doi:10.1021/la015685a
[33] Perkowski J, Bzdon S, Bulska A, et al. Decomposition of detergents present in car-wash sewage by titania photo-assisted oxidation. Polish J Environ Stud. 2006;15:457–465.
[34] Dong H, Zeng G, Tang L, et al. An overview on limitations of TiO_2-based particles for photocatalytic degradation of organic pollutants and the

corresponding countermeasures. Water Res. 2015;79:128–146. doi:10.1016/j.watres.2015.04.038
[35] Wang Y, Vogel A, Sachs M, et al. Current understanding and challenges of solar-driven hydrogen generation using polymeric photocatalysts. Nat Energy. 2019;4:746–760. doi:10.1038/s41560-019-0456-5
[36] Zaleska A. Doped-TiO_2: a review. Recent Patents Eng. 2008;2:157–164. doi:10.2174/187221208786306289
[37] Aguilar T, Navas J, Alcántara R, et al. A route for the synthesis of Cu-doped TiO_2 nanoparticles with a very low band gap. Chem Phys Lett. 2013;571:49–53. doi:10.1016/j.cplett.2013.04.007
[38] Han C, Likodimos V, Khan JA, et al. UV–visible light-activated Ag-decorated, monodisperse TiO_2 aggregates for treatment of the pharmaceutical oxytetracycline. Environ Sci Pollut Res. 2014;21:11781–11793. doi:10.1007/s11356-013-2233-5
[39] Zang Y, Farnood R. Photocatalytic activity of AgBr/TiO_2 in water under simulated sunlight irradiation. Appl Catal B: Environ. 2008;79:334–340. doi:10.1016/j.apcatb.2007.10.019
[40] Hu C, Lan Y, Qu J, et al. Ag/AgBr/TiO_2 visible light photocatalyst for destruction of azodyes and bacteria. J Phys Chem B. 2006;110:4066–4072. doi:10.1021/jp0564400
[41] Arabatzis IM, Stergiopoulos T, Bernard MC, et al. Silver-modified titanium dioxide thin films for efficient photodegradation of methyl orange. Appl Catal B: Environ. 2003;42:187–201. doi:10.1016/S0926-3373(02)00233-3
[42] Fuerte A, Hernández-Alonso MD, Maira AJ, et al. Visible light-activated nanosized doped-TiO_2 photocatalysts. Chem Commun. 2001;24:2718–2719. doi:10.1039/b107314a
[43] Anpo M. Use of visible light. Second-generation titanium oxide photocatalysts prepared by the application of an advanced metal ion-implantation method. Pure Appl Chem. 2000;72:1787–1792. doi:10.1351/pac200072091787
[44] Soria J, Conesa JC, Schiavello M, et al. Dinitrogen photoreduction to ammonia over titanium dioxide powders doped with ferric ions. J Phys Chem. 1991;95:274–282. doi:10.1021/j100154a052
[45] Palmisano L, Schiavello M, Sclafani A, et al. Surface properties of iron-titania photocatalysts employed for 4-nitrophenol photodegradation in aqueous TiO_2 dispersion. Catal Lett. 1994;24:303–315. doi:10.1007/BF00811803
[46] Iliev V, Tomova D, Bilyarska L, et al. Photocatalytic properties of TiO_2 modified with platinum and silver nanoparticles in the degradation of oxalic acid in aqueous solution. Appl Catal B: Environ. 2006;63:266–271. doi:10.1016/j.apcatb.2005.10.014
[47] Khaki MRD, Shafeeyan MS, Raman AAA, et al. Application of doped photocatalysts for organic pollutant degradation - A review. J Environ Manage. 2017;198:78–94. doi:10.1016/j.jenvman.2017.04.099
[48] Chen D, Cheng Y, Zhou N, et al. Photocatalytic degradation of organic pollutants using TiO_2-based photocatalysts: a review. J Clean Prod. 2020;268:121725. doi:10.1016/j.jclepro.2020.121725
[49] Chen D, Jiang Z, Geng J, et al. Carbon and nitrogen Co-doped TiO_2 with enhanced visible-light photocatalytic activity. Ind Eng Chem Res. 2007;46:2741–2746. doi:10.1021/ie061491k
[50] Li X, Wang D, Cheng G, et al. Preparation of polyaniline-modified TiO_2 nanoparticles and their photocatalytic activity under visible light illumination. Appl Catal B: Environ. 2008;81:267–273. doi:10.1016/j.apcatb.2007.12.022
[51] Dong F, Guo S, Wang H, et al. Enhancement of the visible light photocatalytic activity of C-doped TiO_2 nanomaterials prepared by a green synthetic approach. J Phys Chem C. 2011;115:13285–13292. doi:10.1021/jp111916q
[52] Chen X, Liu L, Yu PY, et al. Increasing solar absorption for photocatalysis with black hydrogenated titanium dioxide nanocrystals. Science 2011;331:746–doi:10.1126/science.1200448
[53] Wang Z, Yang C, Lin T, et al. Visible-light photocatalytic, solar thermal and photoelectrochemical properties of aluminium-reduced black titania. Energy Environ Sci. 2013;6:3007. doi:10.1039/c3ee41817k
[54] Zhao Z, Tan H, Zhao H, et al. Reduced TiO_2 rutile nanorods with well-defined facets and their visible-light photocatalytic activity. Chem Commun. 2014;50:2755–2757. doi:10.1039/C3CC49182J
[55] Zou X, Liu J, Su J, et al. Facile synthesis of thermal- and photostable titania with paramagnetic oxygen vacancies for visible-light photocatalysis. Chem Eur J. 2013;19:2866–2873. doi:10.1002/chem.201202833
[56] Kang Q, Cao J, Zhang Y, et al. Reduced TiO_2 nanotube arrays for photoelectrochemical water splitting. J Mater Chem A. 2013;1:5766–5774. doi:10.1039/c3ta10689f
[57] Tominaka S, Tsujimoto Y, Matsushita Y, et al. Synthesis of nanostructured reduced titanium oxide: crystal structure transformation maintaining nanomorphology. Angew Chem Int Ed. 2011;50:7418–7421. doi:10.1002/anie.201101432
[58] Xu C, Song Y, Lu L, et al. Electrochemically hydrogenated TiO_2 nanotubes with improved photoelectrochemical water splitting performance. Nanoscale Res Lett. 2013;8:391. doi:10.1186/1556-276X-8-1
[59] Diebold U. The surface science of titanium dioxide. Surf Sci Rep. 2003;48:53–229. doi:10.1016/S0167-5729(02)00100-0
[60] Chen X, Liu L, Huang F. Black titanium dioxide (TiO_2) nanomaterials. Chem Soc Rev. 2015;44:1861–1885. doi:10.1039/C4CS00330F
[61] Carp O, Huisman CL, Reller A. Photoinduced reactivity of titanium dioxide. Prog Solid State Chem. 2004;32:33–177. doi:10.1016/j.progsolidstchem.2004.08.001
[62] Liu K, Zhu L, Jiang T, et al. Mesoporous TiO_2 micro-nanometer composite structure: synthesis, optoelectric properties, and photocatalytic selectivity. Int J Photoenergy. 2012;2012:849062. doi:10.1155/2012/849062
[63] Mascolo G, Comparelli R, Curri ML, et al. Photocatalytic degradation of methyl red by TiO_2: comparison of the efficiency of immobilized nanoparticles versus conventional suspended catalyst. J Hazard Mater. 2007;142:130–137. doi:10.1016/j.jhazmat.2006.07.068
[64] Weng Y-X, Li L, Liu Y, et al. Surface-binding forms of carboxylic groups on nanoparticulate TiO_2 surface studied by the interface-sensitive transient triplet-state molecular probe. J Phys Chem B. 2003;107:4356–4363. doi:10.1021/jp022534n
[65] Mallakpour S, Nikkhoo E. Surface modification of nano-TiO_2 with trimellitylimido-amino acid-based

diacids for preventing aggregation of nanoparticles. Adv Powder Technol. 2014;25:348–353. doi:10.1016/j.apt.2013.05.017

[66] Nakayama N, Hayashi T. Preparation and characterization of poly(l-lactic acid)/TiO_2 nanoparticle nanocomposite films with high transparency and efficient photodegradability. Polym Degrad Stab. 2007;92:1255–1264. doi:10.1016/j.polymdegradstab.2007.03.026

[67] Uyguner C, Bekbolet M. Application of photocatalysis for the removal of natural organic matter in simulated surface and ground waters. J Adv Oxid Technol. 2016;12:87-92. doi:10.1515/jaots-2009-0110

[68] Matthews RW. Purification of water with near—u.v. illuminated suspensions of titanium dioxide. Water Res. 1990;24:653–660. doi:10.1016/0043-1354(90)90199-G

[69] Deng Y, Qi D, Deng C, et al. Superparamagnetic high-magnetization microspheres with an Fe_3O_4@SiO_2 core and perpendicularly aligned mesoporous SiO_2 shell for removal of microcystins. J Am Chem Soc. 2008;130:28–29. doi:10.1021/ja0777584

[70] Zhang X, Wu F, Deng N. Efficient photodegradation of dyes using light-induced self assembly TiO_2/β-cyclodextrin hybrid nanoparticles under visible light irradiation. J Hazard Mater. 2011;185:117–123. doi:10.1016/j.jhazmat.2010.09.005

[71] Zhang H, Zhu G. One-step hydrothermal synthesis of magnetic Fe_3O_4 nanoparticles immobilized on polyamide fabric. Appl Surf Sci. 2012;258:4952–4959. doi:10.1016/j.apsusc.2012.01.127

[72] Wang S, Zhou S. Titania deposited on soft magnetic activated carbon as a magnetically separable photocatalyst with enhanced activity. Appl Surf Sci. 2010;256:6191–6198. doi:10.1016/j.apsusc.2010.03.139

[73] He Z, Hong T, Chen J, et al. A magnetic TiO_2 photocatalyst doped with iodine for organic pollutant degradation. Sep Purif Technol. 2012;96:50–57. doi:10.1016/j.seppur.2012.05.005

[74] Martyanov IN, Klabunde KJ. Comparative study of TiO_2 particles in powder form and as a thin nanostructured film on quartz. J Catal. 2004;225:408–416. doi:10.1016/j.jcat.2004.04.019

[75] Tang Y, Zhang G, Liu C, et al. Magnetic TiO_2-graphene composite as a high-performance and recyclable platform for efficient photocatalytic removal of herbicides from water. J Hazard Mater. 2013;252–253:115–122. doi:10.1016/j.jhazmat.2013.02.053

[76] Wang C, Yin L, Zhang L, et al. Magnetic $(\gamma\text{-}Fe_2O_3@SiO_2)_n@TiO_2$ functional hybrid nanoparticles with actived photocatalytic ability. J Phys Chem C. 2009;113:4008–4011. doi:10.1021/jp809835a

[77] Makarova OV, Rajh T, Thurnauer MC, et al. Surface modification of TiO_2 nanoparticles for photochemical reduction of nitrobenzene. Environ Sci Technol. 2000;34:4797–4803. doi:10.1021/es001109

[78] Wang Y, Zhang J, Liu X, et al. Synthesis and characterization of activated carbon-coated $SiO_2/TiO_{2-x}C_x$ nanoporous composites with high adsorption capability and visible light photocatalytic activity. Mater Chem Phys. 2012;135:579–586. doi:10.1016/j.matchemphys.2012.05.029

[79] Nguyen-Phan TD, Pham VH, Shin EW, et al. The role of graphene oxide content on the adsorption-enhanced photocatalysis of titanium dioxide/graphene oxide composites. Chem Eng J. 2011;170:226–232. doi:10.1016/j.cej.2011.03.060

[80] Gaya UI, Abdullah AH, Hussein MZ, et al. Photocatalytic removal of 2,4,6-trichlorophenol from water exploiting commercial ZnO powder. Desalination. 2010;263:176–182. doi:10.1016/j.desal.2010.06.055

[81] Zhong N, Chen M, Luo Y, et al. A novel photocatalytic optical hollow-fiber with high photocatalytic activity for enhancement of 4-chlorophenol degradation. Chem Eng J. 2019;355:731–739. doi:10.1016/j.cej.2018.08.167

[82] Yang J, Chen H, Gao J, et al. Synthesis of Fe_3O_4/g-C_3N_4 nanocomposites and their application in the photodegradation of 2,4,6-trichlorophenol under visible light. Mater Lett 2016;164:183–189. doi:10.1016/j.matlet.2015.10.130

[83] Lin JC-T, Sopajaree K, Jitjanesuwan T, et al. Application of visible light on copper-doped titanium dioxide catalyzing degradation of chlorophenols. Sep Purif Technol. 2018;191:233–243. doi:10.1016/j.seppur.2017.09.027

[84] Liu L, Chen F, Yang F, et al. Photocatalytic degradation of 2,4-dichlorophenol using nanoscale Fe/TiO_2. Chem Eng J 2012;181–182:189–195. doi:10.1016/j.cej.2011.11.060

[85] Yang J, Cui S, Qiao JQ, et al. The photocatalytic dehalogenation of chlorophenols and bromophenols by cobalt doped nano TiO_2. J Mol Catal A: Chem. 2014;395:42–51. doi:10.1016/j.molcata.2014.08.001

[86] Shen YS, Ku Y, Lee KC. The effect of light absorbance on the decomposition of chlorophenols by ultraviolet radiation and u.v./H_2O_2 processes. Water Res 1995;29:907–914. doi:10.1016/0043-1354(94)00198-G

[87] Czaplicka M. Photo-degradation of chlorophenols in the aqueous solution. J Hazard Mater. 2006;134:45–59. doi:10.1016/j.jhazmat.2005.10.039

[88] Hinojosa-Reyes M, Camposeco-Solis R, Ruiz F, et al. Promotional effect of metal doping on nanostructured TiO_2 during the photocatalytic degradation of 4-chlorophenol and naproxen sodium as pollutants. Mater Sci Semicond Process. 2019;100:130–139. doi:10.1016/j.mssp.2019.04.050

[89] Long G, Ding J, Xie L, et al. Fabrication of mediator-free g-C_3N_4/Bi_2WO_6Z-scheme with enhanced photocatalytic reduction dechlorination performance of 2,4-DCP. Appl Surf Sci. 2018;455:1010–1018. doi:10.1016/j.apsusc.2018.06.072

[90] Li F, Du P, Liu W, et al. Hydrothermal synthesis of graphene grafted titania/titanate nanosheets for photocatalytic degradation of 4-chlorophenol: solar-light-driven photocatalytic activity and computational chemistry analysis. Chem Eng J. 2018;331:685–694. doi:10.1016/j.cej.2017.09.036

[91] Xu L, Wang J. Degradation of 2,4,6-trichlorophenol using magnetic nanoscaled Fe_3O_4/CeO_2 composite as a heterogeneous Fenton-like catalyst. Sep Purif Technol 2015;149:255–264. doi:10.1016/j.seppur.2015.05.011

[92] Yu J, Wang T, Rtimi S. Magnetically separable TiO_2/FeO_x/POM accelerating the photocatalytic removal of the emerging endocrine disruptor: 2,4-dichlorophenol. Appl Catal B: Environ. 2019;254:66–75. doi:10.1016/j.apcatb.2019.04.088

[93] Peng H, Cui J, Zhan H, et al. Improved photodegradation and detoxification of 2,4,6-trichlorophenol by

lanthanum doped magnetic TiO_2. Chem Eng J. 2015;264:316–321. doi:10.1016/j.cej.2014.11.122

[94] Sinirtas E, Isleyen M, Soylu GSP. Photocatalytic degradation of 2,4-dichlorophenol with V_2O_5-TiO_2 catalysts: effect of catalyst support and surfactant additives. Chin J Catal. 2016;37:607–615. doi:10.1016/S1872-2067(15)61035-X

[95] Li K, Zeng Z, Yan L, et al. Fabrication of C/X-TiO_2@C_3N_4 NTs (X=N, F, Cl) composites by using phenolic organic pollutants as raw materials and their visible-light photocatalytic performance in different photocatalytic systems. Appl Catal B: Environ. 2016;187:269–280. doi:10.1016/j.apcatb.2016.01.046

[96] Ma HY, Zhao L, Guo LH, et al. Roles of reactive oxygen species (ROS) in the photocatalytic degradation of pentachlorophenol and its main toxic intermediates by TiO_2/UV. J Hazard Mater. 2019;369:719–726. doi:10.1016/j.jhazmat.2019.02.080

[97] Ling L, Feng Y, Li H, et al. Microwave induced surface enhanced pollutant adsorption and photocatalytic degradation on Ag/TiO_2. Appl Surf Sci. 2019;483:772–778. doi:10.1016/j.apsusc.2019.04.039

[98] Sharma A, Lee BK. Rapid photo-degradation of 2-chlorophenol under visible light irradiation using cobalt oxide-loaded TiO_2/reduced graphene oxide nanocomposite from aqueous media. J Environ Manage. 2016;165:1–10. doi:10.1016/j.jenvman.2015.09.013

[99] Lan Z, Yu Y, Yan S, et al. Synergetic effect of N^{3-}, In^{3+} and Sn^{4+} ions in TiO_2 towards efficient visible photocatalysis. J Photochem Photobiol A: Chem. 2018;356:132–137. doi:10.1016/j.jphotochem.2017.12.032

[100] Bilgin Simsek E. Solvothermal synthesized boron doped TiO_2 catalysts: photocatalytic degradation of endocrine disrupting compounds and pharmaceuticals under visible light irradiation. Appl Catal B: Environ. 2017;200:309–322. doi:10.1016/j.apcatb.2016.07.016

[101] Chen X, Sun H, Zhang J, et al. Synthesis of visible light responsive iodine-doped mesoporous TiO_2 by using biological renewable lignin as template for degradation of toxic organic pollutants. Appl Catal B: Environ. 2019;252:152–163. doi:10.1016/j.apcatb.2019.04.034

[102] Al-Fahdi T, Al Marzouqi F, Kuvarega AT, et al. Visible light active CdS@TiO_2 core-shell nanostructures for the photodegradation of chlorophenols. J Photochem Photobiol A: Chem. 2019;374:75–83. doi:10.1016/j.jphotochem.2019.01.019

[103] Choi KH, Min J, Park SY, et al. Enhanced photocatalytic degradation of tri-chlorophenol by Fe_3O_4@TiO_2@Au photocatalyst under visible-light. Ceram Int. 2019;45:9477–9482. doi:10.1016/j.ceramint.2018.09.104

[104] Lu YY, Zhang YY, Zhang J, et al. In situ loading of CuS nanoflowers on rutile TiO_2 surface and their improved photocatalytic performance. Appl Surf Sci. 2016;370:312–319. doi:10.1016/j.apsusc.2016.02.170

[105] Mahmiani Y, Sevim AM, Gül A. Photocatalytic degradation of 4-chlorophenol under visible light by using TiO_2 catalysts impregnated with Co(II) and Zn(II) phthalocyanine derivatives. J Photochem Photobiol A: Chem. 2016;321:24–32. doi:10.1016/j.jphotochem.2015.12.015

[106] Zhao X, Wu P, Liu M, et al. Y_2O_3 modified TiO_2 nanosheets enhanced the photocatalytic removal of 4-chlorophenol and Cr (VI) in sun light. Appl Surf Sci. 2017;410:134–144. doi:10.1016/j.apsusc.2017.03.073

[107] Ozturk B, Soylu GSP. Promoting role of transition metal oxide on $ZnTiO_3$-TiO_2 nanocomposites for the photocatalytic activity under solar light irradiation. Ceram Int. 2016;42:11184–11192. doi:10.1016/j.ceramint.2016.04.027

[108] Shojaie A, Fattahi M, Jorfi S, et al. Hydrothermal synthesis of Fe-TiO_2-Ag nano-sphere for photocatalytic degradation of 4-chlorophenol (4-CP): investigating the effect of hydrothermal temperature and time as well as calcination temperature. J Environ Chem Eng. 2017;5:4564–4572. doi:10.1016/j.jece.2017.07.024

[109] Martínez-Sánchez C, Montiel-González F, Díaz-Cervantes E, et al. Unraveling the strength interaction in a TiO_2-graphene photocatalytic nanocomposite synthesized by the microwave hydrothermal method. Mater Sci Semicond Process. 2019;101:262–271. doi:10.1016/j.mssp.2019.06.011

[110] Shoneye A, Tang J. Highly dispersed FeOOH to enhance photocatalytic activity of TiO_2 for complete mineralisation of herbicides. Appl Surf Sci. 2020;511:145479. doi:10.1016/j.apsusc.2020.145479

[111] Saha B, Orvig C. Biosorbents for hexavalent chromium elimination from industrial and municipal effluents. Coord Chem Rev. 2010;254:2959–2972. doi:10.1016/j.ccr.2010.06.005

[112] Pradhan D, Sukla LB, Sawyer M, et al. Recent bioreduction of hexavalent chromium in wastewater treatment: a review. J Ind Eng Chem. 2017;55:1–20. doi:10.1016/j.jiec.2017.06.040

[113] Testa JJ, Grela MA, Litter MI. Heterogeneous photocatalytic reduction of chromium(VI) over TiO_2 particles in the presence of oxalate: involvement of Cr (V) species. Environ Sci Technol. 2004;38:1589–1594. doi:10.1021/es0346532

[114] Wang L, Wang N, Zhu L, et al. Photocatalytic reduction of Cr(VI) over different TiO_2 photocatalysts and the effects of dissolved organic species. J Hazard Mater. 2008;152:93–99. doi:10.1016/j.jhazmat.2007.06.063

[115] Li Y, Bian Y, Qin H, et al. Photocatalytic reduction behavior of hexavalent chromium on hydroxyl modified titanium dioxide. Appl Catal B: Environ. 2017;206:293–299. doi:10.1016/j.apcatb.2017.01.044

[116] Lu D, Zhang G, Wan Z. Visible-light-driven g-C_3N_4/Ti^{3+}-TiO_2 photocatalyst co-exposed {001} and {101} facets and its enhanced photocatalytic activities for organic pollutant degradation and Cr(VI) reduction. Appl Surf Sci. 2015;358:223–230. doi:10.1016/j.apsusc.2015.08.240

[117] Lei XF, Xue XX, Yang H, et al. Visible light-responded C, N and S co-doped anatase TiO_2 for photocatalytic reduction of Cr(VI). J Alloys Compd. 2015;646:541–549. doi:10.1016/j.jallcom.2015.04.233

[118] Petala E, Baikousi M, Karakassides MA, et al. Synthesis, physical properties and application of the zero-valent iron/titanium dioxide heterocomposite having high activity for the sustainable photocatalytic removal of hexavalent chromium in water. Phys Chem Chem Phys. 2016;18:10637–10646. doi:10.1039/C6CP01013J

[119] Wang Q, Shi X, Xu J, et al. Highly enhanced photocatalytic reduction of Cr(VI) on AgI/TiO_2 under visible light irradiation: influence of calcination temperature. J Hazard Mater. 2016;307:213–220. doi:10.1016/j.jhazmat.2015.12.050
[120] Li Y, Cui W, Liu L, et al. Removal of Cr(VI) by 3D TiO_2-graphene hydrogel via adsorption enriched with photocatalytic reduction. Appl Catal B: Environ. 2016;199:412–423. doi:10.1016/j.apcatb.2016.06.053
[121] Mohamed A, Osman TA, Toprak MS, et al. Visible light photocatalytic reduction of Cr(VI) by surface modified CNT/titanium dioxide composites nanofibers. J Mol Catal A: Chem. 2016;424:45–53. doi:10.1016/j.molcata.2016.08.010
[122] Athanasekou C, Romanos GE, Papageorgiou SK, et al. Photocatalytic degradation of hexavalent chromium emerging contaminant via advanced titanium dioxide nanostructures. Chem Eng J. 2017;318:171–180. doi:10.1016/j.cej.2016.06.033
[123] Liu L, Luo C, Xiong J, et al. Reduced graphene oxide (rGO) decorated TiO_2 microspheres for visible-light photocatalytic reduction of Cr(VI). J Alloys Compd. 2017;690:771–776. doi:10.1016/j.jallcom.2016.08.197
[124] Wang L, Zhang C, Gao F, et al. Algae decorated TiO_2/Ag hybrid nanofiber membrane with enhanced photocatalytic activity for Cr(VI) removal under visible light. Chem Eng J. 2017;314:622–630. doi:10.1016/j.cej.2016.12.020
[125] Lei XF, Zhang ZN, Wu ZX, et al. Synthesis and characterization of Fe, N and C tri-doped polymorphic TiO_2 and the visible light photocatalytic reduction of Cr(VI). Sep Purif Technol. 2017;174:66–74. doi:10.1016/j.seppur.2016.09.039
[126] Jiang H, Li M, Liu J, et al. Alkali-free synthesis of a novel heterostructured CeO_2-TiO_2 nanocomposite with high performance to reduce Cr(VI) under visible light. Ceram Int. 2018;44:2709–2717. doi:10.1016/j.ceramint.2017.10.225
[127] Yin R, Ling L, Xiang Y, et al. Enhanced photocatalytic reduction of chromium (VI) by Cu-doped TiO_2 under UV-A irradiation. Sep Purif Technol. 2018;190:53–59. doi:10.1016/j.seppur.2017.08.042
[128] Zhang Y, Xu M, Li H, et al. The enhanced photoreduction of Cr(VI) to Cr(III) using carbon dots coupled TiO_2 mesocrystals. Appl Catal B: Environ. 2018;226:213–219. doi:10.1016/j.apcatb.2017.12.053
[129] Ali I, Kim J-O. Visible-light-assisted photocatalytic activity of bismuth-TiO_2 nanotube composites for chromium reduction and dye degradation. Chemosphere. 2018;207:285–292. doi:10.1016/j.chemosphere.2018.05.075
[130] Wang W, Lai M, Fang J, et al. Au and Pt selectively deposited on {001}-faceted TiO_2 toward SPR enhanced photocatalytic Cr(VI) reduction: the influence of excitation wavelength. Appl Surf Sci. 2018;439:430–438. doi:10.1016/j.apsusc.2017.12.249
[131] Lin W-Y, Wei C, Rajeshwar K. Photocatalytic reduction and immobilization of hexavalent chromium at titanium dioxide in aqueous basic media. J Electrochem Soc. 1993;140:2477–2482, doi:10.1149/1.2220847
[132] Ku Y, Jung I-L. Photocatalytic reduction of Cr(VI) in aqueous solutions by UV irradiation with the presence of titanium dioxide. Water Res. 2001;35:135–142. doi:10.1016/S0043-1354(00)00098-1
[133] Yoon J, Shim E, Bae S, et al. Application of immobilized nanotubular TiO_2 electrode for photocatalytic hydrogen evolution: reduction of hexavalent chromium (Cr(VI)) in water. J Hazard Mater. 2009;161:1069–1074. doi:10.1016/j.jhazmat.2008.04.057
[134] Yin H, Wada Y, Kitamura T, et al. Hydrothermal synthesis of nanosized anatase and rutile TiO_2 using amorphous phase TiO_2. J Mater Chem. 2001;11:1694–1703. doi:10.1039/b008974p
[135] Lu D, Zhao B, Fang P, et al. Facile one-pot fabrication and high photocatalytic performance of vanadium doped TiO_2-based nanosheets for visible-light-driven degradation of RhB or Cr(VI). Appl Surf Sci. 2015;359:435–448. doi:10.1016/j.apsusc.2015.10.138
[136] Lu D, Fang P, Liu X, et al. A facile one-pot synthesis of TiO_2-based nanosheets loaded with Mn_xO_y nanoparticles with enhanced visible light–driven photocatalytic performance for removal of Cr(VI) or RhB. Appl Catal B: Environ. 2015;179:558–573. doi:10.1016/j.apcatb.2015.05.059
[137] Lu D, Chai W, Yang M, et al. Visible light induced photocatalytic removal of Cr(VI) over TiO_2-based nanosheets loaded with surface-enriched CoO_x nanoparticles and its synergism with phenol oxidation. Appl Catal B: Environ. 2016;190:44–65. doi:10.1016/j.apcatb.2016.03.003
[138] Xue C, Zhang T, Ding S, et al. Anchoring tailored low-index faceted BiOBr nanoplates onto TiO_2 nanorods to enhance the stability and visible-light-driven catalytic activity. ACS Appl Mater Interfaces. 2017;9:16091–16102. doi:10.1021/acsami.7b00433
[139] Vellaichamy B, Periakaruppan P, Nagulan B. Reduction of Cr^{6+} from wastewater using a novel in situ-synthesized PANI/MnO_2/TiO_2 nanocomposite: renewable, selective, stable, and synergistic catalysis. ACS Sustain Chem Eng. 2017;5:9313–9324. doi:10.1021/acssuschemeng.7b02324
[140] Choong TSY, Chuah TG, Robiah Y, et al. Arsenic toxicity, health hazards and removal techniques from water: an overview. Desalination. 2007;217:139–166. doi:10.1016/j.desal.2007.01.015
[141] Neppolian B, Doronila A, Grieser F, et al. Simple and efficient sonochemical method for the oxidation of arsenic(III) to arsenic(V). Environ Sci Technol. 2009;43:6793–6798. doi:10.1021/es900878g
[142] Clancy TM, Hayes KF, Raskin L. Arsenic waste management: a critical review of testing and disposal of arsenic-bearing solid wastes generated during arsenic removal from drinking water. Environ Sci Technol. 2013;47:10799–10812. doi:10.1021/es401749b
[143] Arco-Lázaro E, Agudo I, Clemente R, et al. Arsenic (V) adsorption-desorption in agricultural and mine soils: effects of organic matter addition and phosphate competition. Environ Pollut. 2016;216:71–79. doi:10.1016/j.envpol.2016.05.054
[144] Vithanage M, Herath I, Joseph S, et al. Interaction of arsenic with biochar in soil and water: a critical review. Carbon. 2017;113:219-230. doi:10.1016/j.carbon.2016.11.032
[145] Levy IK, Mizrahi M, Ruano G, et al. TiO_2-photocatalytic reduction of pentavalent and trivalent arsenic: production of elemental arsenic and arsine. Environ Sci Technol. 2012;46:2299–2308. doi:10.1021/es202638c
[146] Gannoun C, Turki A, Kochkar H, et al. Elaboration and characterization of sulfated and unsulfated V_2O_5/TiO_2 nanotubes catalysts for chlorobenzene total oxidation. Appl Catal B: Environ. 2014;147:58–64. doi:10.1016/j.apcatb.2013.08.009

[147] Andjelkovic I, Stankovic D, Nesic J, et al. Fe doped TiO_2 prepared by microwave-assisted hydrothermal process for removal of As(III) and As(V) from water. Ind Eng Chem Res. 2014;53:10841–10848. doi:10.1021/ie500849r

[148] Liu W, Zhao X, Borthwick AGL, et al. Dual-enhanced photocatalytic activity of Fe-deposited titanate nanotubes used for simultaneous removal of As(III) and As(V). ACS Appl Mater Interfaces. 2015;7:19726–19735. doi:10.1021/acsami.5b05263

[149] Gao K, Chen J, Liu Z, et al. Intensified redox co-conversion of As(III) and Cr(VI) with MIL-125(Ti)-derived COOH functionalized TiO_2: performance and mechanism. Chem Eng J. 2019;360:1223–1232. doi:10.1016/j.cej.2018.09.134

[150] Gibbs GV, Wallace AF, Cox DF, et al. Role of directed van der Waals bonded interactions in the determination of the structures of molecular arsenate solids. J Phys Chem A. 2009;113:736–749. doi:10.1021/jp807666b

[151] Tang J, Durrant JR, Klug DR. Mechanism of photocatalytic water splitting in TiO_2. Reaction of water with photoholes, importance of charge carrier dynamics, and evidence for four-hole chemistry. J Am Chem Soc. 2008;130:13885–13891. doi:10.1021/ja8034637

[152] Miao TJ, Tang J. Characterization of charge carrier behavior in photocatalysis using transient absorption spectroscopy. J Chem Phys. 2020;152:194201. doi:10.1063/5.0008537